Closed-Form Correlation Model of Oriented Bandpass Natural Images

Che-Chun Su, *Student Member, IEEE*, Lawrence K. Cormack, and Alan C. Bovik, *Fellow, IEEE*

***Abstract*—Most prevalent statistical models of natural images characterize only the univariate distributions of divisively normalized bandpass responses or wavelet-like decompositions of them. However, the higher-order dependencies between spatially neighboring responses are not yet well understood. Towards filling this gap, we propose a new closed-form spatial-oriented correlation model that captures statistical regularities between perceptually decomposed natural image luminance samples. We validate the new correlation model on a variety of natural images. Experimental results demonstrate the robustness of the new correlation model across image content. A software release that implements the new closed-form spatial-oriented correlation model is available at http://live.ece.utexas.edu/research/3dnss/bicorr_release.zip.**

***Index Terms*—Bivariate model, closed-form, natural scene statistics (NSS), spatial-oriented correlation model.**

I. Introduction

MODELING natural scene statistics (NSS) and understanding the low-level human vision system have come to be regarded as a dual problem [2]. NSS models have also proven to be important ingredients towards the design of image/video processing and computer vision algorithms [3]–[6].

A variety of natural scene statistical models have been developed in the vision science literature, both in the spatial [7] and wavelet domain [8]. Early on, Ruderman [7] showed that a simple non-linear operation of local mean subtraction followed by variance divisive normalization on natural image luminance results in a decorrelating and Gaussianizing effect. While the statistics, i.e., marginal distributions, of natural image pixels exhibit non-Gaussian behavior, after projection onto appropriate multi-scale spaces, e.g., using wavelet bases [9] or 2D Gabor filter banks [8], the resulting coefficients are found to obey regular statistical models, such as Gaussian scale mixtures [10]. These natural scene statistical models have been deployed in perceptual and computational image/video applications with great success, such as image denoising and restoration [3], and image/video quality assessment [11]–[14].

However, efforts to date have focused on the use of first-order univariate statistical models, although there certainly exist significant dependencies between spatially neighboring bandpass image responses, which are not yet fully understood or modeled. Some early work has been conducted on analyzing and modeling joint/bivariate relationships between sub-band natural image coefficients. For example, Portilla *et al.* [15], [16] proposed a Markov statistical descriptor for texture images using a set of parametric constraints on pairs of complex wavelet coefficients at adjacent spatial locations, orientations, and scales. In [17], [18], the authors found that the coefficients of orthonormal wavelet decompositions of natural images are fairly well-decorrelated; however, they are not independent. The authors also showed that the empirical joint histograms of adjacent coefficients produce contour plots having distinct 'bowtie' shapes. This was observed on coefficient pairs separated by different spatial offsets, across adjacent scales, and at orthogonal orientations. Liu *et al.* [19] measured inter- and intra-scale dependencies between image wavelet coefficients using mutual information. In [20], Sendur *et al.* considered image wavelet coefficients and their parents (at adjacent coarser scale locations), and proposed a circularly symmetric bivariate distribution to model their dependencies. Po *et al.* [21] applied a two-dimensional contourlet transform to natural images, and examined both the marginal and joint distributions. They measured the dependencies between image contourlet coefficients using mutual information, and proposed a hidden Markov tree (HMT) image model with Gaussian mixtures that can capture interlocation, interscale, and interdirection dependencies. The authors of [22] proposed an infinitely divisible model of generic image statistics, which presupposes that the environment may be subdivided into local objects cast against an ergodic image field, while also containing regions of very little information (e.g., blue sky). However, among all these and other efforts to characterize the bivariate behavior of natural image fields, none has offered a closed-form quantitative model of the bivariate correlations of bandpass natural images. If available, such a closed-form expression could be invaluable for analyzing statistical image behavior and for formulating easily expressed and computed optimized solutions to a wide variety of image processing problems.

Here we make progress towards filling this gap by introducing a new closed-form correlation model of spatially neighboring bandpass natural image responses across sub-band orientations. We start by analyzing bivariate joint histograms using a versatile multivariate generalized Gaussian distribution, and propose a new exponentiated cosine function model of spatial-oriented correlation. We statistically validate the robustness of the new closed-form NSS model.

II. Spatial-Oriented Correlation Natural Scene Statistical Model

Human vision systems (HVS) extract abundant information from natural environments by processing visual stimuli through different levels of decomposition and interpretation. Since we

Manuscript received May 02, 2014; revised July 02, 2014; accepted July 23, 2014. Date of publication August 07, 2014; date of current version August 19, 2014. The associate editor coordinating the review of this manuscript and approving it for publication was Dr. Oscar C. Au.

C.-C. Su and A. C. Bovik are with the Laboratory for Image and Video Engineering (LIVE), Department of Electrical and Computer Engineering, The University of Texas at Austin, Austin, TX 78712 USA (e-mail: ccsu@utexas.edu; bovik@ece.utexas.edu).

L. K. Cormack is with the Department of Psychology, the Center for Perceptual Systems, and the Institute for Neuroscience, The University of Texas at Austin, Austin, TX 78712, USA (e-mail: cormack@utexas.edu).

Color versions of one or more of the figures in this paper are available online at http://ieeexplore.ieee.org.

Digital Object Identifier 10.1109/LSP.2014.2345765

want to learn and explore the statistical relationships that are embedded in natural images, and how these statistics might be implicated in visual processing and used for practical image processing, we apply certain perceptually relevant pre-processing steps on natural image luminance, and develop our new correlation model from the empirical response distributions.

The basic resources on which we perform bivariate and correlation statistical modeling are the pristine images from the popular and widely used LIVE IQA Database [23].

A. Perceptual Decomposition

We acquire luminance by transforming pristine color images into the perceptually relevant CIELAB color space, which is optimized to quantify perceptual color differences and better corresponds to human color perception than does the perceptually nonuniform RGB space [24]. Each luminance image (L^*) is then transformed by the steerable pyramid decomposition, which is an over-complete wavelet transform that allows for increased orientation selectivity [25]. The use of the wavelet transform is motivated by the fact that its space-scale-orientation decomposition is similar to models of the bandpass responses of simple cells in primary visual cortex [8], [26], [27].

After applying the multi-scale, multi-orientation decomposition, we perform the perceptually significant process of divisive normalization on the luminance wavelet coefficients of all of the sub-bands [18]. The divisive normalization transform (DNT) used in our work is implemented as follows [28]:

$$u(x_i, y_i) = \frac{w(x_i, y_i)}{\sqrt{s + \mathbf{w}_\mathbf{g}^\top \mathbf{w}_\mathbf{g}}} = \frac{w(x_i, y_i)}{\sqrt{s + \sum_j g(x_j, y_j) w(x_j, y_j)^2}} \quad (1)$$

where (x_i, y_i) are spatial coordinates, w are the wavelet coefficients, u are the coefficients after DNT, s is a semi-saturation constant, the weighted sum occurs over a spatial neighborhood of pixels indexed by j at the same sub-band, and $\{g(x_j, y_j)\}$ is a finite-extent Gaussian weighting function.

B. Bivariate Joint Distribution Analysis

Before introducing the new correlation model, we start by studying the bivariate joint distribution of spatially adjacent luminance wavelet coefficients subjected to DNT, i.e., u in Eq. (1). Specifically, we use the steerable pyramid decomposition with five scales, indexed from 1 (finest) to 5 (coarsest), and twelve frequency-tuning orientations (defined as the normal to a sinusoidal wave front): $0, \frac{1}{12}\pi, \ldots, \frac{11}{12}\pi$.

Here we mainly focus on the bivariate distributions and correlations of horizontally and vertically adjacent pixels. Specifically, for horizontally adjacent pixels, we sample pairs from locations (x, y) and $(x + 1, y)$ in an image. Since we have observed that very similar statistics arise from horizontally and vertically adjacent pixels, we will only discuss the results for the horizontal case.

To model the bivariate joint histogram of spatially adjacent bandpass responses, we utilize a multivariate generalized Gaussian distribution (MGGD), which includes both the multivariate Gaussian and Laplace distributions as special cases. The use of MGGD is motivated by the fact that the univariate generalized Gaussian distribution has been widely used in modeling univariate natural scene statistics [12], [13]. MGGD is also a versatile and accurate tool for modeling multi-dimensional image histograms [29]. The probability density function of a multivariate generalized Gaussian distribution that we use is:

$$p(\mathbf{x}; \mathbf{M}, \alpha, \beta) = \frac{1}{|\mathbf{M}|^{\frac{1}{2}}} g_{\alpha,\beta}(\mathbf{x}^\top \mathbf{M}^{-1} \mathbf{x}) \quad (2)$$

where $\mathbf{x} \in \mathbb{R}^N$, $\mathbf{M}$ is an $N \times N$ symmetric scatter matrix, α and β are scale and shape parameters, respectively, and $g_{\alpha,\beta}(\cdot)$ is the density generator:

$$g_{\alpha,\beta}(y) = \frac{\beta \Gamma\left(\frac{N}{2}\right)}{\left(2^{\frac{1}{\beta}} \pi \alpha\right)^{\frac{N}{2}} \Gamma\left(\frac{N}{2\beta}\right)} e^{-\frac{1}{2}\left(\frac{y}{\alpha}\right)^\beta} \quad (3)$$

where $y \in \mathbb{R}^+$. Note that when $\beta = 0.5$, Eq. (2) yields the multivariate Laplacian distribution, and when $\beta = 1$, Eq. (2) corresponds to the multivariate Gaussian distribution.

We model the bivariate empirical histograms of horizontally adjacent sub-band coefficients in natural images as following a bivariate generalized Gaussian distribution (BGGD), *viz*., using Eq. (2) with $N = 2$. The BGGD parameters are obtained using the maximum likelihood estimator (MLE) algorithm described in [30].

Fig. 1 shows the empirical joint distributions of horizontally adjacent sub-band responses and their corresponding BGGD fits on pristine image 'building2' from the LIVE IQA Database [23]. The bivariate joint distributions are obtained by first binning both responses at spatially adjacent locations, for example, the responses at location (x, y) and $(x + 1, y)$, to form a two-dimensional grid, then counting the number of occurrences within each grid entry, and finally computing the height of each grid entry by normalizing its occurrence by the sum of occurrences from all entries. As may be seen in the three-dimensional illustrations shown in the top row, where the blue bars represent the actual histograms and the colored meshes represent the BGGD fits, the joint distributions of L^* sub-band responses are well modeled as bivariate generalized Gaussian. The 2D illustrations, which depict iso-probability contour maps of the joint distributions and the fits in the middle and bottom rows, respectively, also demonstrate the close fits of the BGGD model. The most important observation here is that both the shape and height of the bivariate distributions and fits vary with the tuning orientations of the sub-band responses. In particular, when the spatial relationship between bandpass samples, e.g., horizontal, matches the sub-band tuning orientation, e.g., $\frac{1}{2}\pi$, then the joint distribution becomes peaky and extremely elliptical, meaning the horizontally adjacent bandpass responses are highly correlated at sub-band orientation $\frac{1}{2}\pi$. Conversely, when the spatial relationship and the sub-band tuning orientation are orthogonal, e.g., horizontal and 0 (rad), then the joint distribution becomes nearly a circular Gaussian, implying almost uncorrelated sub-band responses.

To further examine this spatial orientation dependency, in Fig. 2(a) we plotted the BGGD model parameters, i.e., α and β, as a function of relative orientation at the same scale as in Fig. 1. Here we define relative orientation as the difference between the sub-band tuning orientation and the spatial orientation of adjacent responses. Fig. 3 demonstrates the definition of the spatial orientation between adjacent pixels. For example, if the sub-band tuning orientation is 0 (rad), and the pixels are horizontally adjacent, i.e., the spatial orientation is $\frac{1}{2}\pi$, then the corresponding relative orientation is equal to $0 - \frac{1}{2}\pi = -\frac{1}{2}\pi$. Fig. 2(a) clearly shows that there is strong orientation dependency of both parameters. We have also studied the behavior of the correlation coefficients of spatially adjacent responses as a function of relative orientation. These are contained in the scatter matrix $\mathbf{M}$ of the BGGD model (Eq. (2) with $N = 2$). Fig. 2(b) shows the correlation coefficients between horizontally adjacent bandpass responses as a function of relative orientation. The horizontally adjacent bandpass responses are most correlated when the sub-band tuning orientation aligns at $\frac{1}{2}\pi$, and become

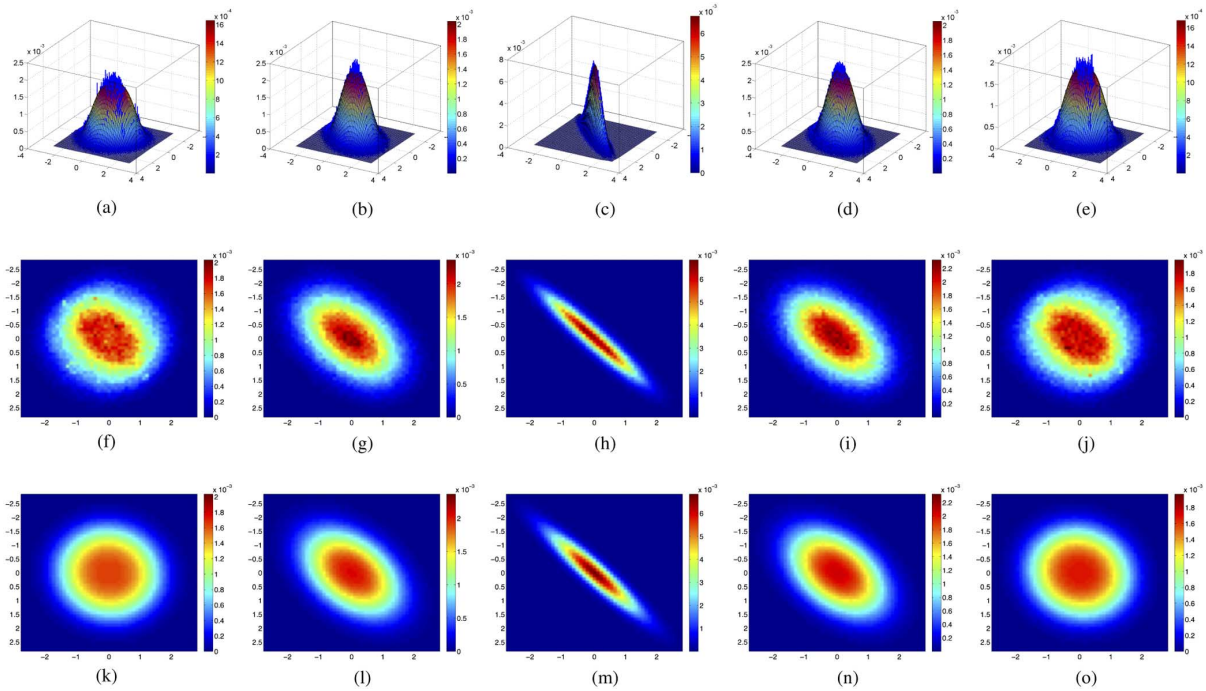

Fig. 1. Joint histograms of horizontally adjacent bandpass coefficients from a pristine image and the corresponding BGGD fits at the finest scale with different orientations. From left column to right column: 0 (rad), $\frac{1}{4}\pi$, $\frac{1}{2}\pi$, $\frac{3}{4}\pi$, and $\frac{11}{12}\pi$. Top row: 3D illustration of bivariate histogram and BGGD fit, middle row: 2D iso-probability contour plot of histogram, and bottom row: 2D iso-probability contour plot of BGGD fit (a) 0(rad) (b) $\frac{1}{4}\pi$ (c) $\frac{1}{2}\pi$ (d) $\frac{3}{4}\pi$ (e) $\frac{11}{12}\pi$ (f) 0(rad) (g) $\frac{1}{4}\pi$ (h) $\frac{1}{2}\pi$ (i) $\frac{3}{4}\pi$ (j) $\frac{11}{12}\pi$ (k) 0(rad) (l) $\frac{1}{4}\pi$ (m) $\frac{1}{2}\pi$ (n) $\frac{3}{4}\pi$ (o) $\frac{11}{12}\pi$.

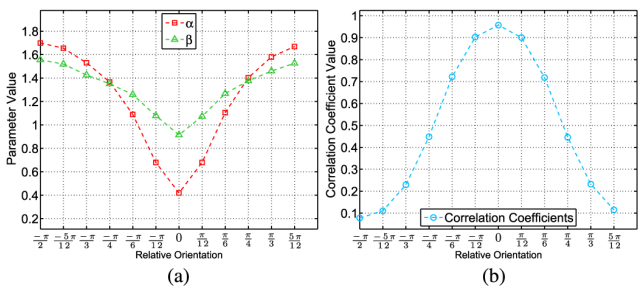

Fig. 2. Plots of the two BGGD model parameters and the correlation coefficients as a function of relative orientation. (a) BGGD parameters. (b) Correlation Coefficients.

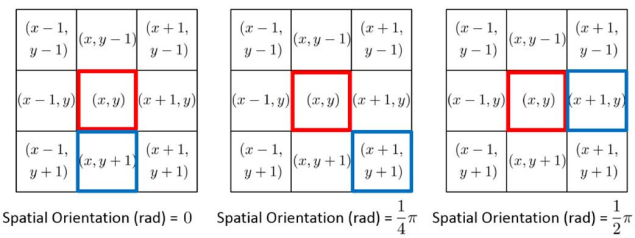

Fig. 3. Definition of the spatial orientation between adjacent pixels, where the red boxes represent the current pixel and the blue boxes represent the spatially adjacent pixels.

nearly uncorrelated at orientations 0 (rad) and π, substantiating the spatial relative orientation dependency observed in Fig. 1.

C. Closed-Form Spatial-Oriented Correlation Model

Motivated by this observed regular, periodic behavior, we have deployed an exponentiated cosine function to model the correlation coefficients as a function of relative orientation:

$$\rho = f(\theta_1, \theta_2) = A\left[\frac{1+\cos\left(2(\theta_2-\theta_1)\right)}{2}\right]^{\gamma} + c \tag{4}$$

$$= A[\cos(\theta_2-\theta_1)]^{2\gamma} + c \tag{5}$$

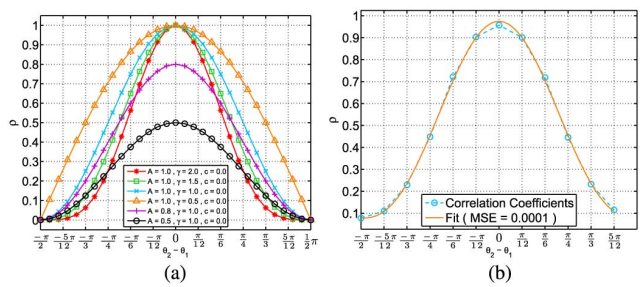

Fig. 4. The exponentiated cosine function and its fit to correlation coefficients as a function of relative orientation (a) Exponentiated cosine function (b) Fit to correlation coefficients.

where ρ is the correlation coefficients between spatially adjacent bandpass responses, θ_1 and θ_2 represent spatial and sub-band tuning orientations, respectively, A is the amplitude, γ is the exponent, and c is the offset. Note that the correlation coefficient ρ is period-π in relative orientation and reaches maximum value when $\theta_2 - \theta_1 = k\pi, k \in \mathbb{Z}$. Fig. 4(a) shows exemplar exponentiated cosine curves for different sets of parameters. The exponentiated cosine model is able to capture a wide range of periodic curves having bell-shaped lobes of varying relative slopes. Fig. 4(b) plots an empirical correlation coefficient curve as a function of relative orientation and its overlaid exponentiated cosine fit for horizontally adjacent bandpass responses, i.e., $\theta_1 = \frac{1}{2}\pi$. From both the curve overlap and associated mean squared error (MSE), it is apparent that the exponentiated cosine model fits the spatial-oriented correlations between adjacent bandpass luminance responses extremely well.

To gain more insight into this exponentiated cosine model, we computed the correlation coefficients between horizontally adjacent bandpass responses as a function of sub-band tuning orientation for all 29 pristine images in the LIVE IQA Database, and found the corresponding exponentiated cosine model parameters,

TABLE I
CHI-SQUARED STATISTICAL TEST RESULTS

Scale	Model Parameter γ	Within-Database Validation on LIVE IQA Database			Cross-Database Validation on VCL@FER Database		
		χ^2	p-value	$> \alpha = 0.05$?	χ^2	p-value	$> \alpha = 0.05$?
1	1.2515	14.6661	0.1983	Yes	16.3808	0.1276	Yes
2	1.2691	8.3057	0.6857	Yes	16.0024	0.1410	Yes
3	1.1846	16.4710	0.1245	Yes	18.0470	0.0805	Yes
4	1.1491	16.1336	0.1362	Yes	14.8301	0.1904	Yes
5	1.1759	9.9386	0.5359	Yes	12.3717	0.3364	Yes

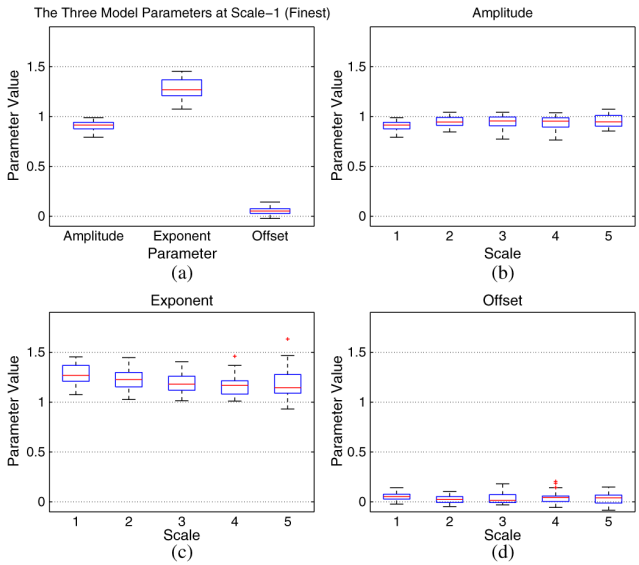

Fig. 5. Box plots of the exponentiated cosine model parameters (a) At the finest scale (b) Amplitude across scales (c) Exponent across scales (d) Offset across scales.

i.e., amplitude A, exponent γ, and offset c. In Fig. 5(a), we present box plots of the three model parameters at the finest scale across all pristine images with whiskers expressing the 1.5 interquartile range (IQR). Fig. 5(b) to (d) show the box plots of amplitude, exponent, and offset obtained from all pristine images across different scales, respectively. Clearly, both the amplitude and offset parameters hold fairly consistent values across image content and scales, i.e., $A \approx 0.9$ and $c \approx 0.05$, while the exponent parameter varies roughly within the range of $[1, 1.4]$, in agreement with the scale-invariant property of natural images [31]. Indeed, little is lost and simplicity gained by taking $A = 1$ and $c = 0$, wherein a succinct one-parameter model may be arrived at:

$$\rho = f(\theta_1, \theta_2; \gamma) = [\cos(\theta_2 - \theta_1)]^{2\gamma} \tag{6}$$

In each of (5)–(6), the model parameters were estimated with non-linear least squares using the Levenberg-Marquardt algorithm [32].

III. VALIDATION OF THE EXPONENTIATED COSINE MODEL

To validate the robustness of the new spatial-oriented correlation model (Eq. (6)), we performed a statistical hypothesis test on the 29 pristine images in the LIVE IQA Database and the 23 pristine images in the VCL@FER Database [33]. In particular, we used a chi-squared statistical test for goodness of fit. First, we computed the exponentiated cosine model parameter γ at each scale by fitting the mean correlation coefficients between horizontally adjacent bandpass responses as a function of sub-band tuning orientation for all LIVE pristine images. Then, we obtained the corresponding exponentiated cosine function, i.e., $\boldsymbol{\rho}_\gamma \in \mathbb{R}^D$ where D is the number of sub-band tuning orientations, using Eq. (6). Finally, we computed the chi-squared statistic χ^2 to determine whether the null hypothesis H_0 is supported, i.e., that the correlation coefficients as a function of sub-band tuning orientation are drawn from a population with mean equal to $\boldsymbol{\rho}_\gamma$. Specifically, if H_0 is rejected, it means that the exponentiated cosine function is not a statistically robust model for natural spatial-oriented correlations; otherwise, we can conclude that the spatial-oriented correlations of all LIVE pristine images can be statistically represented by the exponentiated cosine model $\boldsymbol{\rho}_\gamma$. The chi-squared statistic χ^2 is computed as:

$$\chi^2 = \sum_{i=1}^{N} \sum_{j=1}^{D} \frac{(\rho_{i_j} - \rho_{\gamma_j})^2}{\rho_{\gamma_j}} \tag{7}$$

where $\{\rho_{\gamma_j}\} = \boldsymbol{\rho}_\gamma \in \mathbb{R}^D$ is the model, $\{\rho_{i_j}\} = \boldsymbol{\rho}_i \in \mathbb{R}^D$ are the correlation coefficients as a function of sub-band tuning orientation for the i-th pristine image, and N is the number of pristine images. We also performed a chi-squared statistical test of the exponential cosine model derived from the LIVE IQA Database on the VCL@FER Database, where $\{\rho_{i_j}\} = \boldsymbol{\rho}_i \in \mathbb{R}^D$ are the correlation coefficients for the i-th pristine image in the VCL@FER Database. We repeated this procedure to perform chi-squared statistical tests on all five scales, from 1 (finest) to 5 (coarsest). The test results for both the within- and cross-database validations are summarized in Table I. We can see that the p-values for all five scales are larger than a significance level $\alpha = 0.05$, indicating that the new spatial-oriented exponentiated cosine correlation model holds well for the tested natural images. We also performed the same chi-squared statistical test of the exponential cosine model derived from the VCL@FER Database, and both the within- and cross-database (on the LIVE IQA Database) validations show similar results, which are not included in this paper due to the page limit. Interested readers may refer to [34]. In addition, the model parameter γ estimated for each scale varies slightly around 1.2, which supports the box plot of γ in Fig. 5(c).

IV. CONCLUSION

We have proposed a new closed-form natural scene statistical model that express the correlations between spatially neighboring bandpass responses of natural images across sub-band orientations. The new model was statistically validated as able to model the relative spatial-oriented correlations of natural luminance images. More importantly, our model is perceptually relevant to models of visual processing in human vision systems (HVS), and nearly identical results can be attained using different color space conversions, e.g., YUV, or scale-orientation decompositions, e.g., Gabor [26]. We believe that the new correlation model will prove useful in a broad spectrum of image and video processing algorithms. For example, both the bivariate GGD and the exponentiated cosine models are closed-form, and can be readily used to develop analytic optimization solutions for image denoising, restoration, and enhancement.

REFERENCES

[1] C.-C. Su, "Software release: Bivariate and spatial-oriented correlation models of natural images," [Online]. Available: http://live.ece.utexas.edu/research/3dnss/bicorr_release.zip

[2] W. S. Geisler, "Visual perception and the statistical properties of natural scenes," *Ann. Rev. Psychol.*, vol. 59, no. 1, pp. 167–192, Jan. 2008.

[3] J. Portilla, V. Strela, M. J. Wainwright, and E. P. Simoncelli, "Image denoising using scale mixtures of Gaussians in the wavelet domain," *IEEE Trans. Image Process.*, vol. 12, no. 11, pp. 1338–1351, Nov. 2003.

[4] Z. Wang and A. C. Bovik, "Reduced- and no-reference image quality assessment: The natural scene statistic model approach," *IEEE Signal Process. Mag.*, vol. 28, no. 6, pp. 29–40, Nov. 2011.

[5] H. Tang, N. Joshi, and A. Kapoor, "Learning a blind measure of perceptual image quality," in *Proc. IEEE Conf. Comput. Vis. Pattern Recogn.*, Jun. 2011, pp. 305–312.

[6] A. Bovik, "Automatic prediction of perceptual image and video quality," *Proc. IEEE*, vol. 101, no. 9, pp. 2008–2024, Sep. 2013.

[7] D. L. Ruderman and W. Bialek, "Statistics of natural images: Scaling in the woods," *Phys. Rev. Lett.*, vol. 73, pp. 814–817, Aug. 1994.

[8] D. J. Field, "Relations between the statistics of natural images and the response properties of cortical cells," *J. Opt. Soc. Amer. A*, vol. 4, no. 12, pp. 2379–2394, 1987.

[9] A. Srivastava, A. B. Lee, E. P. Simoncelli, and S.-C. Zhu, "On advances in statistical modeling of natural images," *J. Math. l Imag. Vis.*, vol. 18, no. 1, pp. 17–33, 2003.

[10] S. Lyu and E. P. Simoncelli, "Statistical modeling of images with fields of gaussian scale mixtures," *Adv. Neural Inf. Process. Syst.*, vol. 19, p. 945, 2007.

[11] K. Seshadrinathan and A. C. Bovik, "Motion tuned spatio-temporal quality assessment of natural videos," *IEEE Trans. Image Process.*, vol. 19, no. 2, pp. 335–350, Feb. 2010.

[12] A. K. Moorthy and A. C. Bovik, "Blind image quality assessment: From natural scene statistics to perceptual quality," *IEEE Trans. Image Process.*, vol. 20, no. 12, pp. 3350–3364, Dec. 2011.

[13] A. Mittal, A. K. Moorthy, and A. C. Bovik, "No-reference image quality assessment in the spatial domain," *IEEE Trans. Image Process.*, vol. 21, no. 12, pp. 4695–4708, Dec. 2012.

[14] A. Mittal, R. Soundararajan, and A. Bovik, "Making a "completely blind" image quality analyzer," *IEEE Signal Process. Lett.*, vol. 20, no. 3, pp. 209–212, Mar. 2013.

[15] J. Portilla and E. P. Simoncelli, "Texture modeling and synthesis using joint statistics of complex wavelet coefficients," in *Proc. IEEE Workshop Statist. Comput. Theories of Vis.*, Jun. 1999, vol. 12.

[16] J. Portilla and E. Simoncelli, "A parametric texture model based on joint statistics of complex wavelet coefficients," *Int. J. Comput. Vis.* , vol. 40, no. 1, pp. 49–70, Oct. 2000.

[17] E. P. Simoncelli, "Modeling the joint statistics of images in the wavelet domain," in *Proc. SPIE, Wavelet Applicat. Signal Image Process. VII*, Oct. 1999, vol. 3813, pp. 188–195.

[18] M. J. Wainwright, O. Schwartz, and E. P. Simoncelli, "Natural image statistics and divisive normalization: Modeling nonlinearity and adaptation in cortical neurons," in *Probabilistic Models of the Brain: Perception and Neural Function*. Cambridge, MA, USA: MIT Press, Feb. 2002, pp. 203–222.

[19] J. Liu and P. Moulin, "Information-theoretic analysis of interscale and intrascale dependencies between image wavelet coefficients," *IEEE Trans. Image Process.*, vol. 10, no. 11, pp. 1647–1658, Nov. 2001.

[20] L. Sendur and I. Selesnick, "Bivariate shrinkage functions for wavelet-based denoising exploiting interscale dependency," *IEEE Trans. Signal Process.*, vol. 50, no. 11, pp. 2744–2756, Nov. 2002.

[21] D.-Y. Po and M. Do, "Directional multiscale modeling of images using the contourlet transform," *IEEE Trans. Image Process.*, vol. 15, no. 6, pp. 1610–1620, Jun. 2006.

[22] D. Mumford and B. Gidas, "Stochastic models for generic images," *Quarterly Appl. Math.*, vol. 59, no. 1, pp. 85–112, Mar. 2001.

[23] H. R. Sheikh, Z. Wang, L. K. Cormack, and A. C. Bovik, LIVE Image Quality Assessment Database, [Online]. Available: http://live.ece.utexas.edu/research/quality/subjective.htm

[24] U. Rajashekar, Z. Wang, and E. P. Simoncelli, "Perceptual quality assessment of color images using adaptive signal representation," in *Proc. SPIE Int. Conf. Human Vis. Electron. Imag.*, Jan. 2010, vol. 7527, no. 1.

[25] E. P. Simoncelli and W. T. Freeman, "The steerable pyramid: A flexible architecture for multi-scale derivative computation," in *Proc. IEEE Int. Conf. Image Process.*, Oct. 1995, vol. 3, pp. 444–447.

[26] M. Clark and A. C. Bovik, "Experiments in segmenting texton patterns using localized spatial filters," *Pattern Recogn.*, vol. 22, no. 6, pp. 707–717, 1989.

[27] B. A. Olshausen and D. J. Field, "How close are we to understanding V1?," *Neural Comput.*, vol. 17, no. 8, pp. 1665–1699, Aug. 2005.

[28] S. Lyu, "Dependency reduction with divisive normalization: Justification and effectiveness," *Neural Comput.*, vol. 23, pp. 2942–2973, 2011.

[29] F. Pascal, L. Bombrun, J.-Y. Tourneret, and Y. Berthoumieu, "Parameter estimation for multivariate generalized Gaussian distributions," *IEEE Trans. Signal Process.*, vol. 61, no. 23, pp. 5960–5971, Dec. 2013.

[30] C.-C. Su, L. K. Cormack, and A. C. Bovik, "Bivariate statistical modeling of color and range in natural scenes," in *Proc. SPIE, Human Vis. Electron. Imag. XIX*, Feb. 2014, vol. 9014.

[31] D. J. Field, "Scale-invariance and self-similar 'wavelet' transforms: An analysis of natural scenes and mammalian visual systems," in *Wavelets, Fractals, and Fourier Transforms: New Developments and New Applications*. Oxford, U.K.: Oxford Univ. Press, 1993, pp. 151–193.

[32] D. W. Marquardt, "An algorithm for least-squares estimation of nonlinear parameters," *J. Soc. for Ind. Appl. Math.*, vol. 11, no. 2, pp. 431–441, 1963.

[33] A. Zaric, N. Tatalovic, N. Brajkovic, H. Hlevnjak, M. Loncaric, E. Dumic, and S. Grgic, "VCL@FER image quality assessment database," in *Proc. ELMAR*, Sep. 2011, pp. 105–110.

[34] C.-C. Su, L. K. Cormack, and A. C. Bovik, "Validation of the exponentiated cosine model," [Online]. Available: http://live.ece.utexas.edu/research/3dnss/bicorr.html